The “polar vortex” winter of 2013/14

Cohen, J. ORCID: https://orcid.org/0000-0002-7762-4482, Agel, L., Barlow, M. ORCID: https://orcid.org/0000-0002-7612-3811, Furtado, J. C. ORCID: https://orcid.org/0000-0001-6580-2109, Kretschmer, M. ORCID: https://orcid.org/0000-0002-2756-9526 and Wendt, V. ORCID: https://orcid.org/0000-0003-1806-4507 (2022) The “polar vortex” winter of 2013/14. Journal of Geophysical Research: Atmospheres, 127 (17). e2022JD036493. ISSN 2169-8996 doi: 10.1029/2022jd036493 Available at https://reading-pure-test.eprints-hosting.org/107049/

JGR Atmospheres

RESEARCH ARTICLE
10.1029/2022JD036493

The "Polar Vortex" Winter of 2013/2014

Judah Cohen[1,2], Laurie Agel[3], Mathew Barlow[3], Jason C. Furtado[4], Marlene Kretschmer[5], and Vivien Wendt[6]

[1]Atmospheric and Environmental Research, Inc, Lexington, MA, USA, [2]Department of Civil and Environmental Engineering, Massachusetts Institute of Technology, Cambridge, MA, USA, [3]Environmental, Earth, and Atmospheric Sciences, University of Massachusetts Lowell, Lowell, MA, USA, [4]School of Meteorology, University of Oklahoma, Norman, OK, USA, [5]Department of Meteorology, University of Reading, Reading, UK, [6]Department of Solar-Terrestrial Physics, German Aerospace Center, Neustrelitz, Germany

Key Points:

- The media attributed the extreme cold in winter 2013/2014 to polar vortex variability though no sudden stratospheric warmings occurred
- The polar vortex did repeatedly stretch that winter, which favors relatively cold temperatures east of the Rockies
- The stretching of the polar vortex and wave amplification was related to wave reflection of upward propagating Rossby waves from Asia

Supporting Information:

Supporting Information may be found in the online version of this article.

Correspondence to:

J. Cohen,
jcohen@aer.com

Citation:

Cohen, J., Agel, L., Barlow, M., Furtado, J. C., Kretschmer, M., & Wendt, V. (2022). The "polar vortex" winter of 2013/2014. *Journal of Geophysical Research: Atmospheres*, *127*, e2022JD036493. https://doi.org/10.1029/2022JD036493

Received 14 JAN 2022
Accepted 8 AUG 2022

Author Contributions:

Conceptualization: Judah Cohen
Formal analysis: Judah Cohen, Laurie Agel, Mathew Barlow, Jason C. Furtado, Marlene Kretschmer, Vivien Wendt
Writing – original draft: Judah Cohen
Writing – review & editing: Judah Cohen, Laurie Agel, Mathew Barlow, Jason C. Furtado, Marlene Kretschmer, Vivien Wendt

Abstract The term "polar vortex" remained largely a technical term until early January 2014 when the United States (US) media used it to describe an historical cold air outbreak in eastern North America. Since then, "polar vortex" has been used more frequently by the media and the public, often conflating circulation features and temperatures near the surface with only partially related features at the tropopause and in the stratosphere. The polar vortex in its most common scientific usage refers to a hemispheric-scale stratospheric circulation over the Arctic that is present during the Northern Hemisphere cold season. Reversal of the zonal mean zonal winds circumnavigating the stratospheric polar vortex (SPV), termed major sudden stratospheric warmings, can be linked to mid-latitude cold air outbreaks. However, this mechanism does not explain the cold US winter of 2013/2014. This study revisits the winter of 2013/2014 to understand how SPV variability may still have played a role in the severe winter weather. Observations indicate that anomalously strong vertical wave propagation occurred throughout the winter and disrupted, but did not fully break, the SPV. Instead, vertically propagating waves were reflected back downward, amplifying a blocking high near Alaska and downstream troughing across central North America, a classic signature for extreme cold air outbreaks across central and eastern North America. Thus, the association of the term "polar vortex" with winter 2013/2014, while not justified by the most common usage of the term, serves as a case study of the wave-reflection mechanism of SPV influence on mid-latitude weather.

Plain Language Summary During the record cold North American winter of 2013/2014, the media introduced the "polar vortex" to the public to much confusion. We show that the polar vortex in the stratosphere was indeed intimately related to the extreme cold observed that winter but not in the classical sense of so-called major sudden stratospheric warmings, which denote a complete breakdown of the polar vortex. Instead, the anomalous cold was related to stretching or an elongation of the polar vortex (more recently identified as "reflective" events). This mechanism resulting in an elongated polar vortex is related to wave amplification and therefore to extreme cold across North America. Our case study of the winter 2013/2014 shows the importance of the polar vortex for weather patterns not previously considered and can help improve predicting extreme winter weather.

1. Introduction

There have been a surprising number of cold winters across North America compared to model projections over the past 20 years resulting in a winter cooling trend in central North America since 2009 (Cohen et al., 2020). The North American cooling peaked during the winter of 2013/2014 (Baxter & Nigam, 2015; Harada & Hirooka, 2017; Hartmann, 2015; Sigmond and Fyfe, 2016). For example, the central United States (US) experienced its coldest winter (December through February) since 1978/1979 (NOAA National Centers for Environmental Information) and Chicago recorded its coldest December through March period on record (dating back to 1872) during that winter (NWS, 2014). The cold temperatures in eastern North America in recent years coincided with anomalous warm and dry conditions in western North America (Singh et al., 2016). This temperature dipole of relatively warm and dry conditions across western North America with relatively cold and wet conditions in eastern North America during winter 2013/2014 was one of the strongest since 1980 (Singh et al., 2016).

The media used the term "polar vortex" for the first-time during winter 2013/2014 in an effort to provide attribution to the anomalous cold (e.g., CBS News, 2014; NOAA, 2014; NY Times, 2019; Waugh et al., 2017).

According to the Glossary of Meteorology from the American Meteorological Society, the term "polar vortex" describes a planetary-scale mid-to high-latitude circumpolar circulation in both the troposphere and the stratosphere. It can also refer to smaller-scale vortices that usually occur within the circumpolar circulation in polar regions near the tropopause (called tropopause polar vortices; Shapiro et al., 1987). In the scientific literature, association of the term polar vortex with anomalously cold weather is often following a significant disruption or weakening of the stratospheric polar vortex (SPV). These disruptions of the SPV are characterized by rapid warming of the polar stratosphere and are referred to as major sudden stratospheric warmings (SSWs; defined when the zonal mean zonal wind at 60°N, 10 hPa reverses from positive to negative or from westerly to easterly, signifying a complete breakdown of the SPV; e.g., Charlton & Polvani, 2007). SPV variability projects onto the leading pattern of extratropical geopotential height variability (Baldwin & Dunkerton, 1999, 2001; Polvani and Kushner, 2002; Thompson and Wallace, 2000), which in the troposphere represents meridional oscillations of atmospheric mass between high-and mid-latitudes and is termed the Arctic Oscillation (AO) or Northern Annular Mode (NAM; e.g., Baldwin, 2001; Gong & Wang, 1999; Namias, 1950; Thompson and Wallace, 1998, 2000; Thompson et al., 2002). In the stratosphere, the NAM serves as a proxy for the strength of the SPV (e.g., Thompson and Wallace, 2000). The negative phase of the tropospheric NAM is related to an increase in the likelihood of colder and snowier weather in large parts of the mid-latitudes during winter (e.g., Cohen et al., 2015; Thompson and Wallace, 2001).

Large disruptions of the SPV result in a negative stratospheric NAM which is often followed by a negative NAM in the troposphere and can persist for up to 60 days following the initial stratospheric perturbation (e.g., Baldwin & Dunkerton, 2001). However, no dates from the winter of 2013/2014 are included in the compendium of major SSW events (Butler et al., 2017; ESRL, 2020). These observations led to confusion in using the term polar vortex among scientists and in the media (ABC News, 2014; AIR, 2014; Manney et al., 2022; Waugh et al., 2017).

The apparent contradiction between the anomalously cold US winter of 2013/2014 and the lack of significantly large SPV disruptions that winter motivated investigating other modes of SPV variability. Kretschmer, Coumou et al. (2018), Kretschmer, Cohen et al. (2018), and Matthias and Kretschmer (2020) expanded upon previous work (e.g., Kodera et al., 2008, 2016; Nath et al., 2014; Perlwitz and Harnik, 2003, 2004; Shaw et al., 2010) and showed that the influence of SPV variability on US weather is more complex than a binary mode of positive and negative NAM. Cluster analysis of SPV variability in the mid-stratosphere identified SSWs characterized by large geopotential height rises centered over the pole as the weakest state of SPV variability (Kretschmer, Coumou et al., 2018). However, cluster analysis of lower stratospheric geopotential heights for the months of January and February also identified alternate weak SPV behavior with more regional geopotential height rises—that is over eastern Siberia and Alaska (Kretschmer, Cohen, et al., 2018). In addition, rather than a displacement or splitting of the SPV, the SPV undergoes a distortion in its shape, with more of a horizontal stretching from a quasi-circular shaped circulation with the center mostly confined to the Arctic to a more elliptical circulation with a center that extends from Asia to North America (their cluster four). Cohen et al. (2021) repeated the cluster analysis and identified SPV stretching events in all months of October through February.

Differences between these two distinct modes of SPV variability reside in the characteristic wave driving patterns associated with stratospheric circulation anomalies. Indeed, prior to and even during breakdowns of the SPV, wave activity is absorbed in the polar stratosphere. In contrast, for the so-called "stretched" SPV events, waves are reflected or redirected off reflective surfaces in the polar stratosphere and returned into the troposphere (Kodera et al., 2008, 2016; Kretschmer, Cohen, et al., 2018; Nath et al., 2014; Perlwitz and Harnik, 2004).

The formation of these reflective surfaces occurs when wave activity flux (WAF; Plumb, 1985) converges in the polar stratosphere leading to a deceleration of the zonal winds in the mid to upper stratosphere while winds remain strong at lower altitudes, creating a reflective surface for the waves (Kodera et al., 2008). Since WAF is reflected during these events they are also referred to as "reflecting" events in the scientific literature (Kodera et al., 2008, 2013, 2016).

Another difference between the two clusters is the associated tropospheric response. The tropospheric response to an SSW is the "classic," well-documented negative tropospheric NAM response that lags up to 2 weeks after the SSW and can last for up to 60 days (e.g., Baldwin & Dunkerton, 2001; Domeisen, Grams, & Papritz, 2020). Also, the largest surface temperature response is across northern Eurasia (Kretschmer, Coumou et al., 2018). In contrast, the tropospheric response to a reflective SPV event is characterized by a negative North Pacific

Oscillation (NPO; Linkin and Nigam, 2008; Rogers, 1981) with a blocking high near Alaska and relatively cold temperatures across much of Canada and the eastern US (Kodera et al., 2013; Lee et al., 2019). Additionally, the tropospheric response is usually instantaneous to the reflected WAF and is of relatively short duration, lasting on the order of days and up to 2 weeks (Matthias and Kretschmer, 2020) as opposed to weeks to months following major SSWs (Baldwin & Dunkerton, 2001). Finally, North American cold anomalies are found to be most intense during and immediately after reflective SPV events (Kretschmer, Cohen, et al., 2018; Lee et al., 2019). This study explores whether the SPV played a role in the extreme winter weather across North America during the winter of 2013/2014. The working hypothesis is that, despite the lack of a major SSW that winter, frequent upward wave propagation into the polar stratosphere contributed to a persistently disturbed and occasionally weak SPV that generated reflective layers for subsequent upward propagating waves. These reflected waves, in turn, supported the anomalously amplified circulation pattern across North America that produced the record cold winter conditions in central North America. In other words, we show that the use of the term "polar vortex" to explain the cold extremes that winter can be justified, yet not in the originally intended usage by the media.

Previously discussed wave reflection events in the scientific literature focused on downward wave activity or reversed poleward heat flux associated with wave-1 over the polar cap (Dunn-Sigouin & Shaw, 2015, 2018; Shaw and Perlwitz, 2013; Shaw et al., 2014). These reflective events are associated with a shift toward a positive AO or North Atlantic Oscillation, a poleward shifted North Atlantic storm track and relatively mild temperatures across the mid-latitudes but especially Europe that can characterize an entire winter (Dunn-Sigouin & Shaw, 2015, 2018; Perlwitz and Harnik, 2003, 2004; Shaw and Perlwitz, 2013; Shaw et al., 2014). As an example, we show a canonical example of reflection from February 2020 (see Figure S1 in Supporting Information S1) where upward WAF is followed by downward WAF, a circular SPV and a mid-troposphere circulation that is characterized by below normal geopotential heights across the entire Arctic but especially in the North Atlantic sector with above normal geopotential heights across the mid-latitudes.

The frequency of reflective events may be sensitive to the quasi-biennial oscillation, sea surface temperatures (SSTs) including in the North Atlantic and El Niño/Southern Oscillation (ENSO) regions (Lubis et al., 2016) and changes in greenhouse gasses (Lubis et al., 2018). However, as we will discuss below the wave reflection that characterized the winter of 2013/2014 exhibited important differences from most previously studied wave reflection events.

2. Data and Methods

For all atmospheric fields, we used daily mean fields from the fifth generation of the European Centre for Medium-range Weather Forecasting (ECMWF) atmospheric reanalyzes (ERA-5; Hersbach et al., 2020). ERA-5 data is available hourly on pressure surfaces at a horizontal resolution of 31 km on 137 vertical levels, from the surface up to 0.01 hPa (around 80 km). Anomalies for all daily quantities are derived from the ERA-5 reanalysis by removing the multi-year mean (1980–2017) for each day. Seasonal (November–March) climatology of all the atmospheric fields presented are shown in Figure S2 of Supporting Information S1.

Just as definitions for SSWs are numerous (see Butler et al., 2015), there are different ways to identify stretched/reflective SPV events. Here we follow the recent work of Cohen et al. (2021) relying on cluster analysis for identifying stretched/reflective SPV events. More precisely, for fall and winter 2013/2014 (specifically October–February), we repeat the clustering analysis of Kretschmer, Cohen, et al. (2018) and Cohen et al. (2021) to find all days that are identified as cluster four of the 100-hPa geopotential height anomaly field, which resemble the characteristic spatial pattern of reflective events. Following Matthias and Kretschmer (2020), we also calculate a regional reflective index (RI) as an alternative to cluster analysis for identifying wave reflection events. The RI is defined as the difference between the standardized meridional eddy heat flux over Siberia (120°–185°E) and Canada (225°–300°E) averaged between 45° and 75°N at 100-hPa:

$$\mathrm{RI} = (v'T')^{*}\,\mathrm{Siberia} - (v'T')^{*}\,\mathrm{Canada}$$

where v denotes the meridional wind, T denotes temperature, the prime denotes the deviation from the zonal mean, and the asterisk indicates that the quantities are standardized. When RI is above +1.5 for 10 consecutive days, this is considered a reflective event (Matthias and Kretschmer, 2020).

Moreover, we perform additional wave analysis, including eddy geopotential height, and WAF in the vertical, meridional and zonal directions similar to Kodera et al. (2008, 2016) to select the events that are indeed related to wave reflection. For computing WAF on a sphere ($\mathbf{F}_s$) we followed the derivation of Plumb (1985):

$$F_s = p\cos\varphi\left(v'^2 - \frac{1}{2\Omega a\sin 2\varphi}\frac{\partial(v'\Phi')}{\partial\lambda} - u'v' + \frac{1}{2\Omega a\sin 2\varphi}\frac{\partial(u'\Phi')}{\partial\lambda}\frac{2\Omega\sin\varphi}{S}\left[v'T' - \frac{1}{2\Omega a\sin 2\varphi}\frac{\partial(T'\Phi')}{\partial\lambda}\right]\right)$$

where

$$S = \frac{\partial\hat{T}}{\partial z} + \frac{\kappa\hat{T}}{H}$$

is the static stability, the caret indicates an areal average over the polar cap north of 20°N, p is pressure, u is zonal wind, H is constant scale height, $z = -H\ln p$ is the log-pressure coordinate, Φ is geopotential height, Ω is Earth's rotation rate (7.292×10^{-5} s^{-1}), a is the radius of Earth, ϕ is latitude, and λ is longitude. The vertical component of WAF, WAF$_z$, is filtered to only show waves 1–3, as these waves dominate wave-driving in the Northern Hemisphere polar stratosphere (e.g., Charney & Drazin, 1961; Matsuno, 1970).

There is a question whether the wave energy that initiated the SPV stretching/reflective events analyzed is related to low and/or high frequency waves. We decomposed the tropospheric eddy waves into their low (>10 days) and high (2–7 days) frequencies and found most of the eddy wave energy in the low frequency waves (not shown). We also computed the transient WAF (Plumb, 1986) and found most of the WAF$_z$ is explained by the stationary waves (Plumb, 1985). Therefore, in the rest of the analysis we only used the derivation of WAF provided in Plumb (1985).

Several indices of weather variability and forcing are used in this study. For regional temperature anomalies across North America, we area-averaged (i.e., cosine-weighted) the temperature anomalies for the region bounded by 40°–60°N, 260°–290°E. For the regional 100-hPa WAF$_z$ anomalies over Siberia and Canada, we area-averaged WAF$_z$ fields over 50°–75°N, 120°–185°E, and 50°–75°N, 225°–300°E, respectively. For the North Pacific regional height anomalies, we area-averaged over the region bounded by 50°–75°N, 150°–210°E. For a representative blocking index, we followed the derivation of Tibaldi and Molteni (1990) which detects reversal in the geopotential height gradient:

$$\begin{aligned}\mathrm{GHGS}(\lambda,t) &= \frac{Z(\lambda,\phi_o,t) - Z(\lambda,\phi_s,t)}{\phi_o - \phi_s}\ \mathrm{GHGN}(\lambda,t) = \frac{Z(\lambda,\phi_n,t) - Z(\lambda,\phi_o,t)}{\phi_n - \phi_o}\ \phi_n\\ &= 80°N + \delta\phi_o = 60°N + \delta\phi_s = 40°N + \delta\delta\\ &= -5°, 0°, 5° \quad \text{Criteria for blocking event (1)GHGS} > 0\ \text{(2)GHGN} < -10\end{aligned}$$

where Z is the geopotential height at 500 hPa (subjected to a 5-day running mean) and t is time. We limited our computation of the blocking index to the North Pacific sector bounded by 150°–230°E. We also used an alternate definition of blocking from Dole and Gordon (1983) and found that identified periods of blocking were not sensitive to the blocking definition (see Figure S3 in Supporting Information S1).

Statistical significance is determined for the surface temperature anomalies by comparing the anomalies with the 90th percentile confidence interval of composited anomalies generated by random sampling of 1,000 dates from representative times in the data set (15 November–1 March 1980–2017). For example, for the event beginning 1 February 2014, 1,000 dates are randomly selected, and for each date, the surface temperature anomalies are composited for the period 8–15 days after. At each grid point, the composited event value for 8–15 days after is statistically significant if it is outside the 90th percentile of the 1,000 random composited values.

To test for robustness of our results, we repeated all atmospheric analyses with the National Aeronautics and Space Administration (NASA) Modern Era Retrospective Reanalysis for Research and Application (MERRA-2; Gelaro et al., 2017). The analyses were consistent between ERA-5 and MERRA-2 and in the article, we therefore only show analysis using ERA-5.

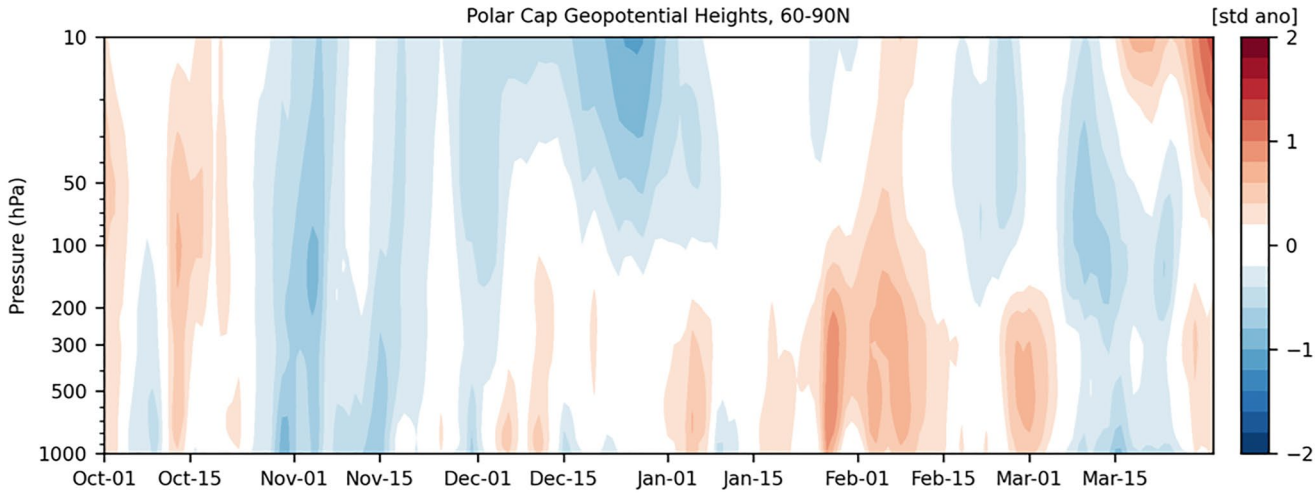

Figure 1. Observed daily polar cap geopotential height (i.e., area-averaged geopotential heights poleward of 60°N) standardized anomalies from 1 October 2013 through 31 March 2014.

3. Results

3.1. Overview of Winter 2013/2014 Weather and Identification of Reflective Events

The winter of 2013/2014 did not feature a strongly negative stratospheric or tropospheric NAM, which is the most common teleconnection index to illustrate stratosphere-troposphere coupling. Figure 1 shows the vertical profile of polar cap height anomalies (i.e., area-averaged geopotential height anomalies poleward of 60°N on isobaric surfaces, a commonly used proxy for the NAM) does not display any downward-propagating NAM signal (i.e., "dripping") from the stratosphere to the troposphere below. As discussed in the Introduction, the anomalously cold periods of the winter of 2013/2014 were unrelated to SSWs or zonal mean SPV disruptions (where the warming is symmetric around the North Pole). However, WAF_z was anomalously positive throughout the stratosphere almost continuously from the end of December 2013 through the end of March 2014 (Figure S4 in Supporting Information S1). This is consistent with Harnik (2009) and Sjoberg and Birner (2012) who demonstrated that upward propagating waves are critical for creating reflective surfaces and Dunn-Sigouin and Shaw (2018) who demonstrated with idealized experiments higher-order waves numbers ($k > 1$) were key to creating the reflecting surfaces. So, while no major SSWs occurred during the winter of 2013/2014, the active WAF_z leaves open the possibility for wave reflection.

In Figure 2a, we show the poleward heat flux $v'T'$, a good proxy for WAF_z, for wave-1 only. During winter 2013/2014 there were periods when $v'T'$ associated with wave-1 was negative (WAF_z is downward) and even record negative, especially in early February, suggestive of wave reflection (e.g., Perlwitz and Harnik, 2003). However, we also show in Figure 2b that $v'T'$ associated with wave-2 was mostly *positive* (WAF_z is upward) and at times *record positive*, especially in early February. In fact, Harada and Hirooka (2017) found that the 2013/2014 winter average of wave-2 WAF_z was one of the highest observed over the reanalysis period. Moreover, the winter average of WAF_z waves one and two shows upward WAF_z over Asia and downward WAF_z over North America (see Figure 2c), characteristic of wave reflection that dominated the winter averages. Furthermore, Harada and Hirooka (2017) observed strong convergence of WAF_z in the region of the stratospheric Aleutian high that favored negative wave refraction in the region (Harada & Hirooka, 2017), which is supportive of wave reflection (Harnik & Lindzen, 2001).

We continue our analysis by characterizing the overall weather conditions in North America during the winter of 2013/2014. Temperatures in eastern North America were almost continuously below average throughout the winter of 2013/2014 with the most notable exception of mid-January (Figure 3, purple line and Figure S5 in Supporting Information S1, blue line). In particular, three prominent periods of below normal temperatures in eastern North America occurred during that winter: (a) mid-November through early January, (b) late January through mid-February and (c) late February into early March.

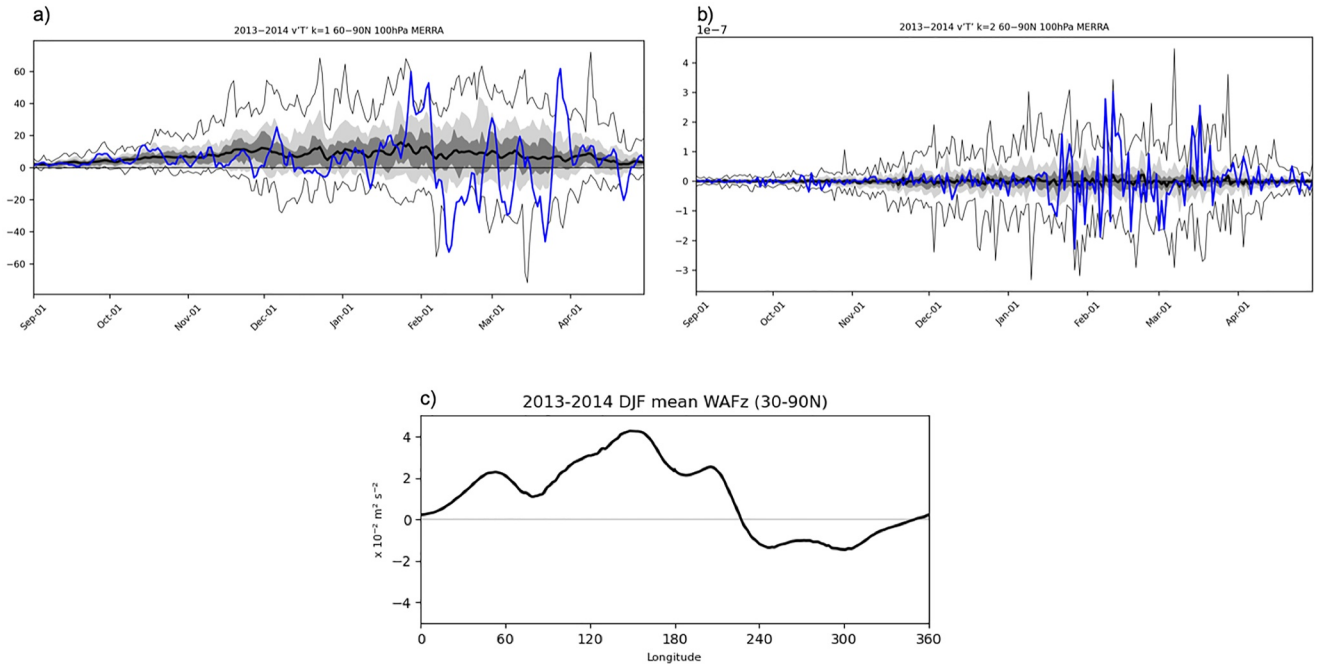

Figure 2. Daily poleward heat flux v'T' at 100 hPa for (a) wave-1 only and (b) wave-2 only averaged 60–90°N. The blue line denotes the timeseries for 2013–2014 (up until the time the figure was made), the black lines denote the climatology, the black shading denotes the 25th–75th percentile range, the gray shading denotes the 10th to 90th percentile range and the gray lines denote the largest positive and negative values in the record. c) Winter mean WAF_z by longitude.

As a first diagnostic to identify reflective events (see Section 2), we perform clustering on the 100-hPa geopotential heights as in Kretschmer, Cohen, et al. (2018) and Cohen et al. (2021). All the dates identified as cluster four are listed in Table 1. Our cluster analysis identifies dates that are synchronous with relatively cold periods in eastern North America suggestive of the relationship between SPV stretching and relatively cold weather that winter. We further compute the RI for the winter of 2013/2014 (Figure S5 in Supporting Information S1 red line). There are three periods when the RI exceeds +1.5: (a) briefly in early November, (b) mid-January to early February and (c) late February to late March. Overall, these two simple 100-hPa diagnostics suggest that wave reflection occurred episodically throughout the winter. These periods of wave reflection also match well with the particularly cold spells across North America noted earlier.

Next, we plot the daily evolution of different indices over the course of the winter of 2013/2014 (Figure 3). Specifically, we compute the WAF_z averaged over Siberia (Figure 3a, blue line), over Canada (Figure 3a, orange line), the geopotential height anomaly over the northern North Pacific at 100 hPa (Figure 3b, magenta line) and at 500 hPa (Figure 3b, green line) and the standardized surface temperature anomaly over eastern North America (Figure 3c, purple line). Based on this analysis, there are five periods that can be characterized as reflective events, identified where the WAF_z is upward over Siberia and downward over Canada (Figure 3a, red arrows). Each reflective event is followed by ridging in the lower stratosphere and mid-troposphere over the North Pacific (Figure 3b, red arrows) and cold temperatures in eastern North America (Figure 3c, red arrows). In addition, the correlation between the North Pacific blocking index and the regional temperature anomalies in eastern North America is strongest and statistically significant at lag 0 and when the blocking index leads by a few days (not shown). Of the five events, based on the clustering analysis (Table 1) and the RI (Figure S5 in Supporting Information S1), the two events that are robustly classified as reflective events are observed from mid-January through mid-February (listed as 8 February 2014) and from late February through mid-March (listed as 4 March 2014).

To further test for evidence of the impact of a reflective event on subseasonal North American weather, we analyze blocking occurrences across the North Pacific (Figures 3a, Figures S3 and S5 in Supporting Information S1) which are linked to cold air outbreaks downstream and often follow reflective events (Harada & Hirooka, 2017; Kodera et al., 2008, 2013). Indeed, pronounced blocking episodes occurred in early November, early December and then 3 times during the winter—in late January, early February and late February into early

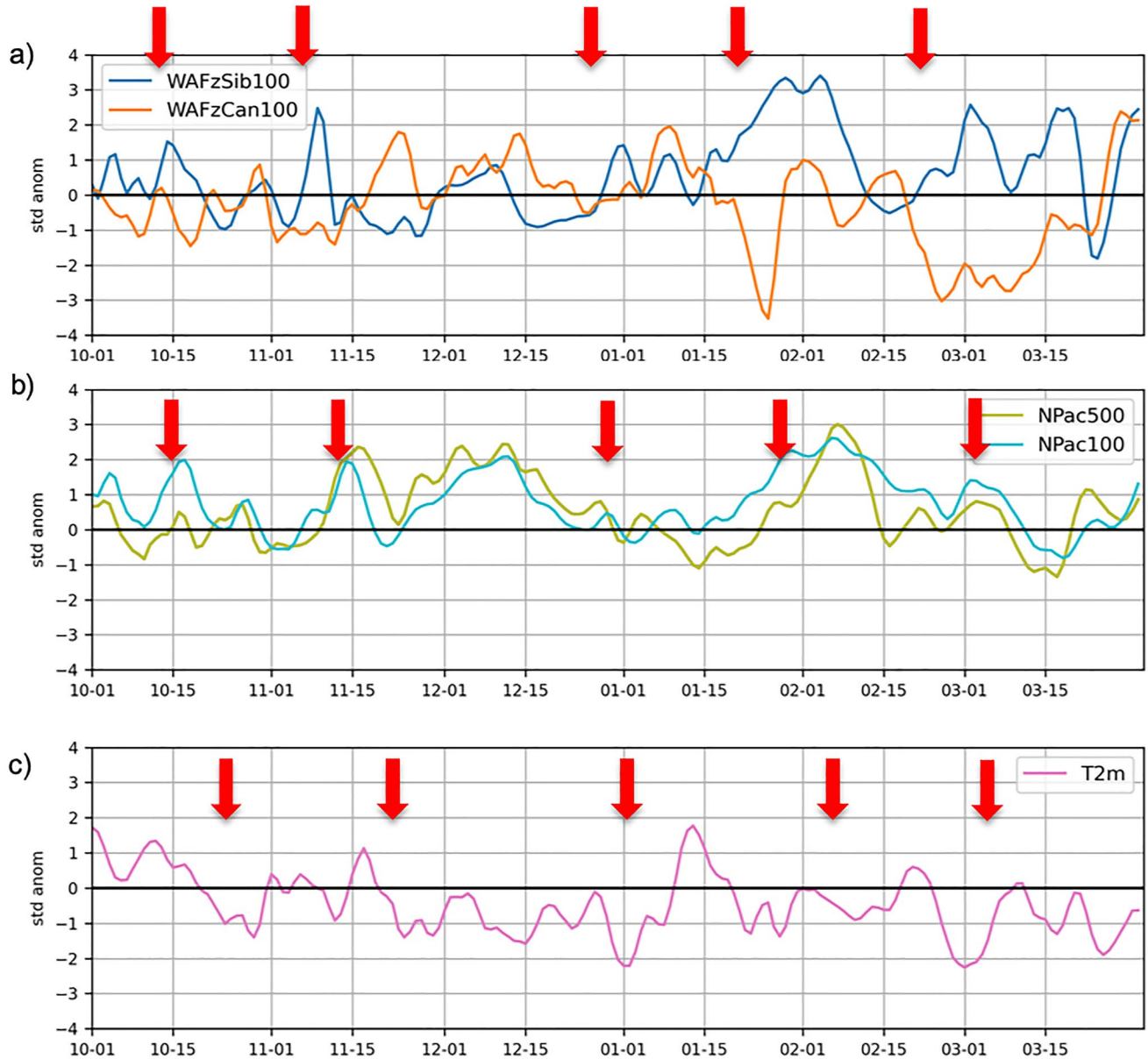

Figure 3. Daily values of (a) area-averaged WAF_z over Siberia (calculated over 50°–75°N, 120°–185°E) and Canada (calculated over 50°–75°N, 225°–300°) and (b) area-averaged geopotential height anomaly at 100 and 500 hPa (calculated over 50°–75°N and 150°–210°E) and (c) area-averaged surface temperature anomalies over the Northeastern USA and Southeastern Canada (40°–60°N, 260°–290°E) over the course of the winter 2013/2014. All values are standardized. The red arrows indicate reflective events defined when WAF_z is upward over Siberia and downward over North America. The red arrows of the same order (first, second, third, etc.) in all the panels represent the same event.

March (Figures 3a, Figures S3 and S5 in Supporting Information S1). These three latter blocking periods approximately coincide with the peaks in the RI in late January into early February and late February into early March (Figure S5 in Supporting Information S1, red shading).

In summary, the different analyses suggest an influence of wave reflection in driving at least two of the cold air outbreaks across North America during the winter of 2013/2014. For the remainder of the study, we focus on the four periods identified as cluster four events in Table 1 and which further exhibit clear wave reflection in Figure 3a: early November, late December into early January, late January into early February and late February into early March. As the latter two events are the most robustly identified reflective events across all metrics, we will begin our analysis on the last two events listed in Table 1. Then we will analyze the period of early November

Table 1
Days From 1 November 2013 Through 31 March 2014 Identified as Cluster Four or Reflective Events

Days identified as cluster four of 100-hPa geopotential height anomalies or reflective events	
First day	Duration in days
7 November 2013	3
5 December 2013	11
19 December 2013	15
5 January 2014	2
9 January 2014	3
16 January 2014	2
8 February 2014	11
4 March 2014	4

Note. Dates in bold are described in more detail in the text.

(listed as 7 November 2013) when the RI only briefly exceeded +1.5. We will conclude the analysis with the cold air outbreak of late December to early January (listed as 5 January 2014) when the term "polar vortex" was mostly widely used and is most closely associated with the weather of that winter.

3.2. Late Winter SPV Reflective Events of 2013/2014

The first robust (across all metrics) reflective event occurred from late January through early February 2014. The event occurred in two parts, and we will focus on the second part in early February when North Pacific blocking peaked for the winter (Figures 3a and Figure S5 in Supporting Information S1). Another reflective event occurred at the end of February and early March with renewed North Pacific blocking (Figures 3a and Figure S5 in Supporting Information S1). Since the two events are similar in character, we will discuss the two events together.

During the first and last weeks of February, WAF in the vertical and meridional directions (WAF_{yz}) was directed upward from the surface through the mid-stratosphere (see arrows in Figures 4a and 4c). During this period, the jet stream in the troposphere was centered between 30 and 35°N and the polar night jet between 60 and 70°N with winds increasing with height in the stratosphere (Figures 4a and 4c, shading). However, as waves broke along the polar night jet, depositing anomalous heat and momentum fluxes, the zonal mean zonal winds weakened during the second week of February and the end of the first week of March (Figures 4b and 4d). As a result, a reflective layer formed in the stratosphere, shown by the negative vertical wind shear, so that WAF was still directed upward between 40 and 55°N but also directed downward between 65 and 80°N (Figures 4b and 4d). The WAF_z at 100 hPa (Figures S6a and S6b in Supporting Information S1, shading) shows the characteristic signature of reflective events with positive (upward) over the Urals and eastern Siberia and negative (downward) over Canada (Kretschmer, Cohen, et al., 2018). We also observe eastward wave propagation originating over the Eurasian sector into the North Pacific and continuing into North America and the North Atlantic (Figures S6a and S6b in Supporting Information S1, vectors).

In Figures 5a and 5c, we show the daily average for 2 and 27 February 2014 of eddy geopotential height anomalies (i.e., the zonal mean removed; shading) along 60°N, WAF in the vertical and zonal directions (WAF_{xz}), and WAF_{xz} convergence. Wave propagation can be observed starting with the anomalous tropospheric ridging near the Urals, then into the East Asian trough, then the North Pacific ridge and finally into the eastern North America and North Atlantic trough. Geopotential height anomalies and WAF in the zonal and meridional directions (WAF_{xy}) at 500 hPa also exhibit general eastward wave propagation (Figures S7a and S7b in Supporting Information S1; vectors).

The WAF_{xyz} shown in Figures 4 and 5 highlights the importance of the troposphere in reflective/SPV stretching events as the primary source of the energy responsible for wave amplification over North America and the resultant cold air outbreaks. The role of the stratosphere is primarily as a reflective layer redirecting WAF_z back down toward the troposphere, resulting in convergence near the tropopause and centered at the Dateline (Figure 5).

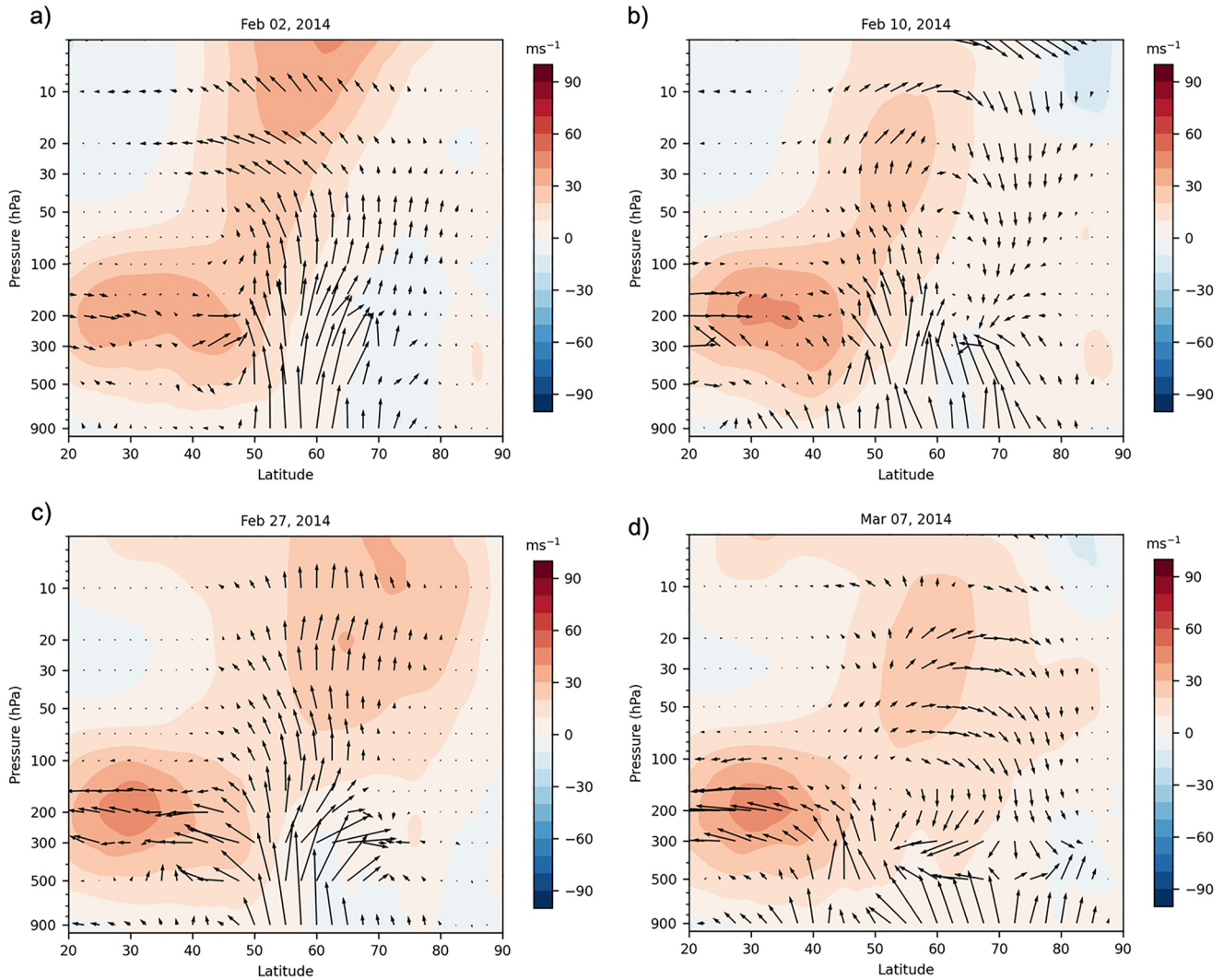

Figure 4. Latitude-height cross section of zonal mean zonal wind and wave activity flux vectors in the longitudinal and height directions from the surface through 10-hPa for (a) 2 February 2014, (b) 10 February 2014, (c) 27 February 2014 and (d) 7 March 2014.

WAF convergence strengthens the North Pacific ridging first in the stratosphere and then in the troposphere (Figures 5a and 5c).

Consistent with upward vertically propagating Rossby waves, the waves in the geopotential heights tilt westward with height over the Eurasian sector. During the second week of February and the first week of March (Figures 5b and 5d), after the formation of the reflective layer, the waves in the geopotential heights tilt eastward with height over eastern North America and the North Atlantic, which is necessary for downward wave propagation (Figures 5b and 5d).

The geopotential heights in the lower stratosphere at 100 hPa during 8–15 February and again 1–7 March 2014 exhibit a strong dipole of a positive height anomaly across the North Pacific side of the Arctic and a negative height anomaly across Eastern Canada and extending into the North Atlantic (Figures 6a and 6d). Consistent with SPV reflective events, a similar dipole is observed at 500-hPa for the same periods (Figures 6b and 6e). This feature is coupled with relatively warm surface temperatures in the North Pacific sector of the Arctic and cold surface temperature anomalies across Canada, the eastern US and large parts of Asia for the second week of February and first week of March (Figures 6c and 6f), as expected during the Alaska ridge regime of Lee et al. (2019).

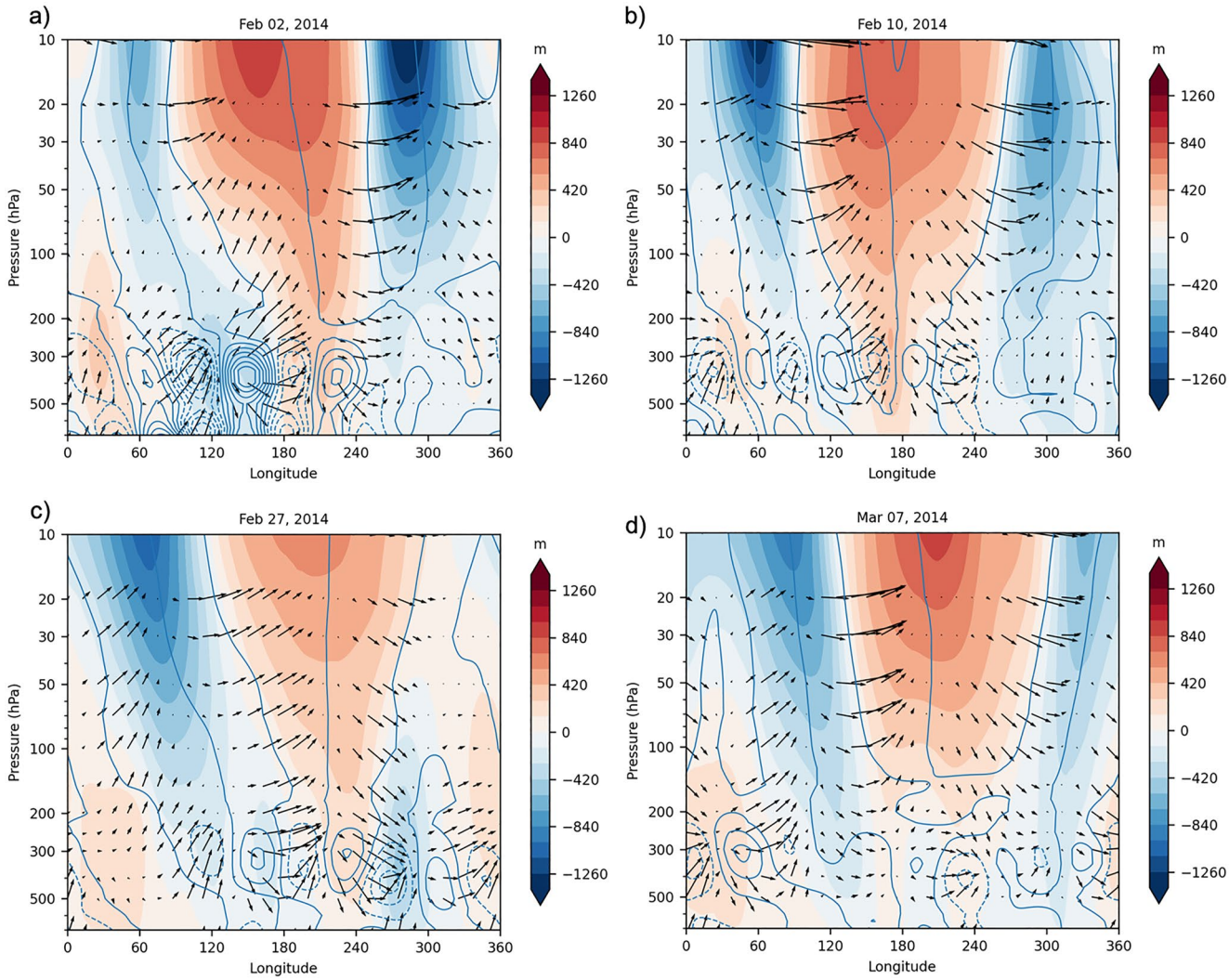

Figure 5. Longitude-height cross section of geopotential eddy height anomalies, wave activity flux (WAF) vectors and convergence (dashed lines) and divergence (solid lines) of WAF in blue contours averaged between 55 and 70°N for (a) 2 February 2014, (b) 10 February 2014, (c) 27 February 2014 and (d) 7 March 2014.

In summary, these two cold air outbreaks show clear signatures of SPV stretching and wave reflection. Analysis of the atmospheric circulation indicates that during that period, waves originated in the troposphere over Eurasia and propagated eastward and upward and eventually downward over North America resulting in convergence of WAF, critical for strengthening tropospheric ridging. This wave propagation in the vertical and longitudinal directions contributed to wave amplification and anomalously cold weather over eastern North America.

3.3. Fall and Early Winter Reflective Events

Next, we analyze whether the cold period from late October through early January might be related to or at least initiated by reflective events identified by the daily analysis shown in Figure 3 (though less distinctive or amplified relative to the later events based on the RI). Though WAF_z in Figure 3a suggests a reflective event in late October, the clustering analysis, the RI, and the North Pacific blocking do not identify a reflective event during this period. Instead, all metrics are more consistent, identifying a reflective event in early November. Since this event occurred in the fall, we discuss it in the Supporting Information S1 (SI).

The next period when an SPV event is identified by clustering analysis, which coincides with active WAF_z (Figure S4 in Supporting Information S1), is late December and early January, the period when the term "polar vortex" was first used by the media to describe the cold air outbreak in early January (Waugh et al., 2017).

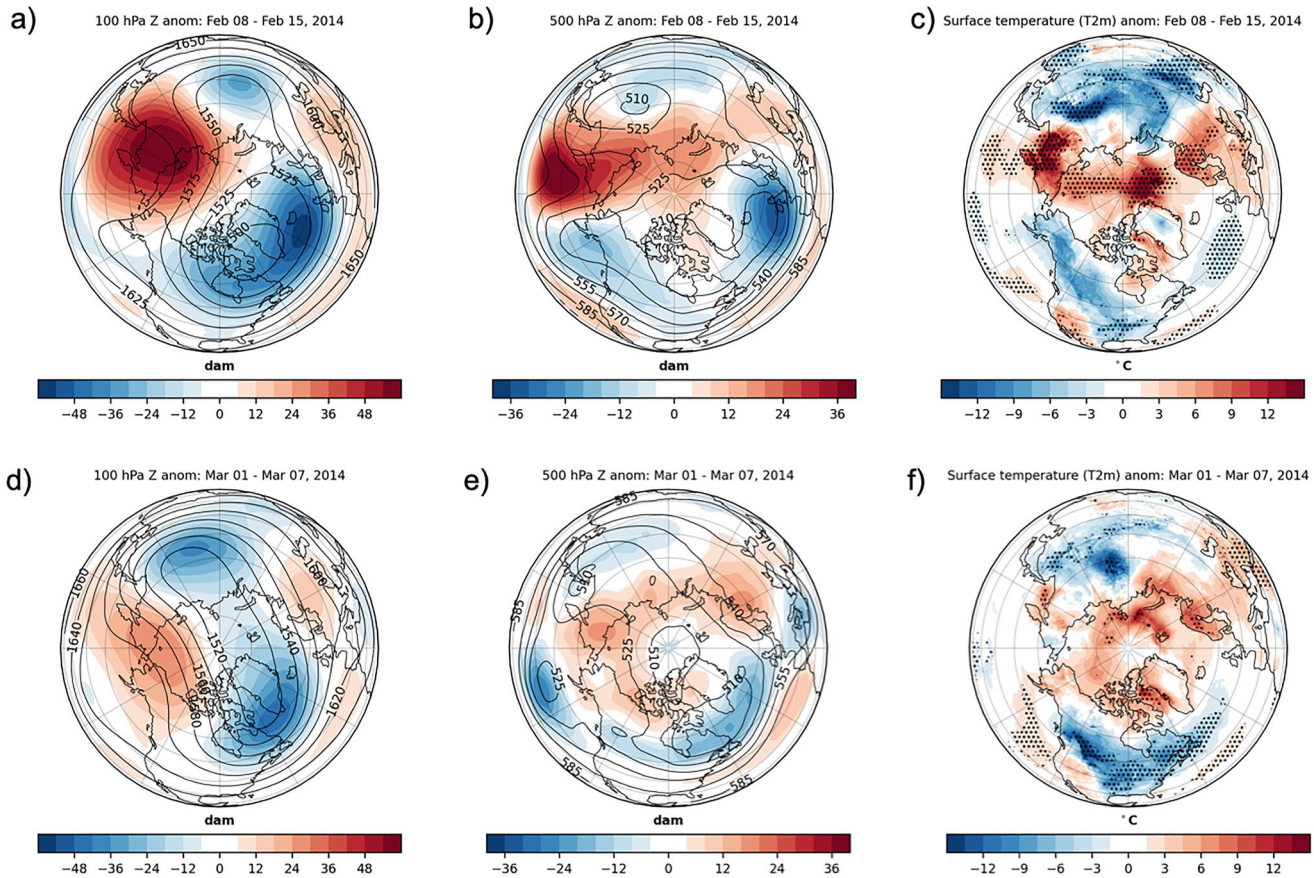

Figure 6. (a) 100-hPa geopotential heights (dam; contours) and geopotential height anomalies (m; shading) from 8 to 15 February 2014, (b) 500-hPa geopotential heights (dam; contours) and geopotential height anomalies from 8 to 15 February 2014 and (c) surface temperature anomalies from 8 to 15 February 2014. (d) through (f) same as (a) through (c) but from 1 to 7 March 2014. Stippling represents 90% significance.

Similar to all three periods of North American cold previously analyzed, an upward and eastward Rossby wave propagation can be seen in the lower stratosphere originating near the Urals, then propagating into the East Asian trough, then into the North Pacific ridging and finally into the eastern North America/North Atlantic troughing (Figure S6d in Supporting Information S1). This same eastward propagating wave energy can be seen in the 500 hPa geopotential height anomaly field and WAF_{xy} (Figure S7d in Supporting Information S1). The observed WAF convergence strengthens the tropospheric ridging over the North Pacific east of the Dateline (Figure 7d).

However, there are notable differences from the late winter reflective events (Section 3b). Though the upward WAF_z in late December 2013 (Figure 7a) and early January 2014 (Figure 7b) resulted in a weakening of the polar night jet, a decrease in the zonal mean zonal wind is not observed in early January. Still, there are signs of reflection (i.e., upward centered at 60°N and downward or at least a downward component in the WAF_z vectors centered at 70°N) but these are shallower and weaker than the reflections that occur later in the winter (Figure 7b). In terms of WAF_z at 100-hPa, there are positive anomalies over northeast Asia and negative anomalies over northwestern North America the last week of December 2013 (Figure S6d in Supporting Information S1) but the anomalies are weaker than those observed in February and March 2014. Convergence of WAF_{xz} was observed in the North Pacific ridging at the end of December 2013 and into early January 2014 (Figures 7c and 7d) amplifying the North American wave.

From 5 to 10 January 2014, there are anomalously positive geopotential heights in the North Pacific at 100-hPa but they do not extend into the Arctic (Figure 8a). Despite less amplified ridging, there are strong negative anomalous geopotential heights in eastern North America (Figure 8a). This pattern is mirrored in the mid-troposphere with a deep trough in eastern North America (Figure 8b) despite a lack of blocking in the North Pacific (Figure S5 in Supporting Information S1). As a result, relatively warm temperatures are observed in eastern Siberia

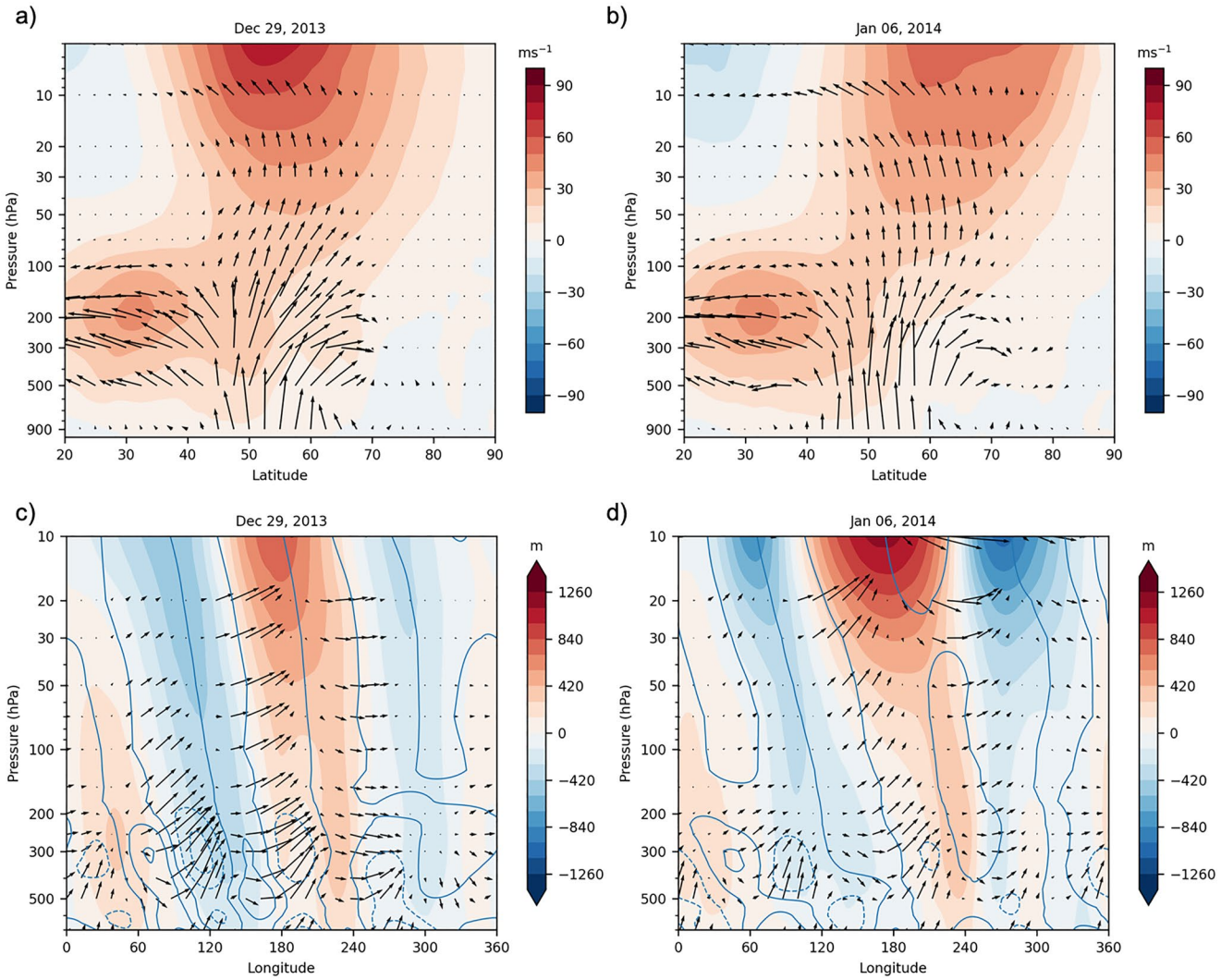

Figure 7. Zonal mean zonal wind and wave activity flux (WAF) vectors in the longitudinal and height directions from the surface through 10 hPa for (a) 29 December 2013 and (b) 6 January 2014. (c and d) same as (a and b) but showing the longitude-height cross section of geopotential eddy height anomalies, WAF vectors and convergence (dashed lines) and divergence (solid lines) of WAF in blue contours.

and Alaska with relatively cold temperatures in eastern Canada and the eastern US (Figure 8c; only statistically significant over the Great Lakes). Negative temperature anomalies are also observed in central Asia and overall, the Northern Hemisphere temperature anomaly pattern closely resembles the Northern Hemisphere temperature anomaly pattern associated with SPV stretching events. So, though the media latched onto this particular event to introduce the term "polar vortex," the relationship between severe winter weather and SPV variability is ironically not as clear as other North American cold air outbreaks that winter.

3.4. Seasonal Analysis of the Stretched SPV Events in Winter 2013/2014 and Their Precursors

Given the recurring and persistent stretched SPV events during the winter of 2013/2014, it is plausible that these synoptic scale events left an imprint on the seasonal means. In fact, winter average (December 2013 through March 2014) anomalies in geopotential heights in the lower stratosphere and mid-troposphere and surface temperatures (Figure 9) resemble the anomalies associated with stretched SPV events (Kretschmer, Cohen, et al., 2018). Strongly positive anomalous geopotential height anomalies in the lower stratosphere are focused in the North Pacific sector of the Arctic with negative geopotential height anomalies across eastern Canada that extend into the northern North Atlantic (Figure 9a). This pattern is mirrored in the mid-troposphere with ridging all along

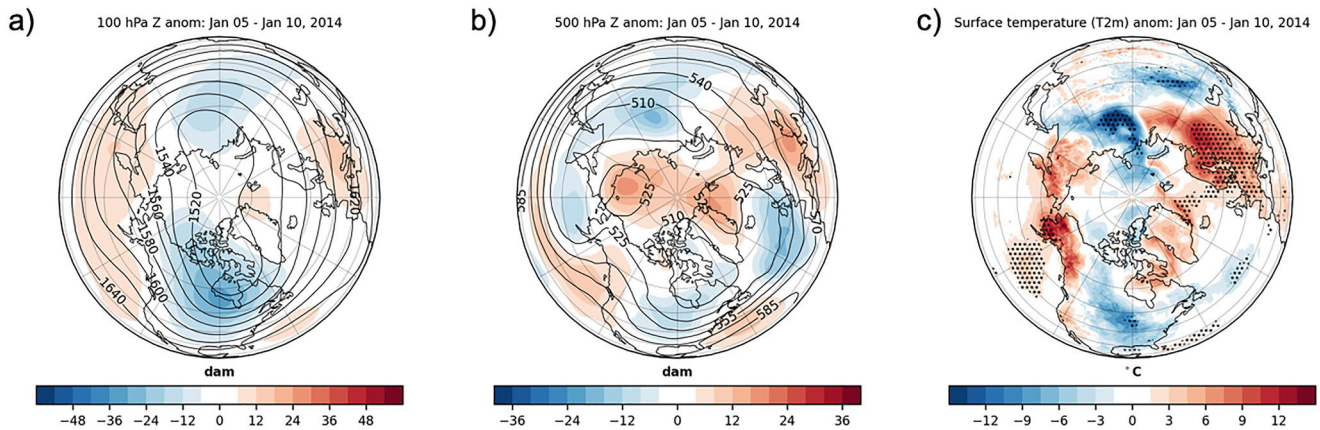

Figure 8. (a) 100-hPa geopotential heights (dam; contours) and geopotential height anomalies (m; shading) from 5 to 10 January 2014, (b) 500-hPa geopotential heights (dam; contours) and geopotential height anomalies from 5 to 10 January 2014 and (c) surface temperature anomalies from 5 to 10 January 2014. Stippling represents 90% significance based on the Student's *t*-test.

the western coast of North America and extending into Alaska, eastern Siberia and into the western Arctic with deep troughing in eastern North America and the northern North Atlantic (Figure 9b). Given the similarity of the tropospheric pattern associated with SPV stretching events with the negative phase of the Pacific/North America pattern associated with La Niña (Horel & Wallace, 1981), we correlated the frequency of SPV stretching days with the winter Oceanic Niño Index (ONI) or ONI index. We found a very weak relationship between the two (see Figure S10 in Supporting Information S1) though more analysis is needed and is beyond the scope of our study.

The anomalous circulation pattern results in positive temperature anomalies in Alaska, Eastern Siberia and Europe and negative temperature anomalies in eastern North America and central Asia (Figure 9c). This temperature anomaly pattern matches the patterns shown in Kretschmer, Cohen, et al. (2018) (their Figure 5), Cohen et al. (2021) (their Figure 1) for stretched SPV events, and Lee et al. (2019) (their Figure 5c) for the Alaska ridge regime. The similarities between these figures suggest that the impacts from the multiple SPV stretching events and subsequent North Pacific blocking significantly contributed to the seasonal averages possibly more so than any other winter in the reanalysis period. Indeed, Kretschmer, Cohen, et al. (2018) found the highest number of reflective event days of any winter in the reanalysis period during the winter of 2013/2014.

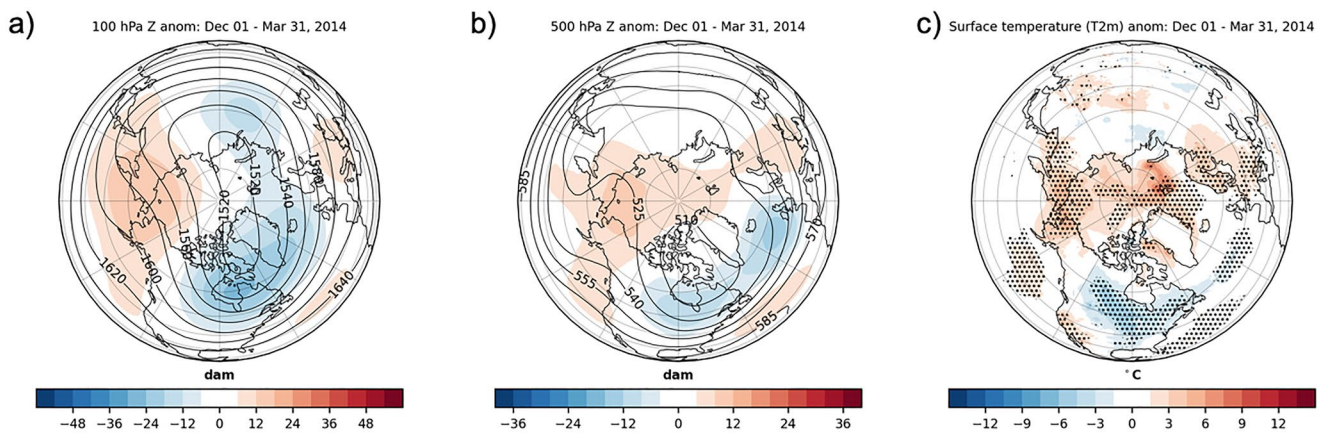

Figure 9. (a) 100-hPa geopotential heights (dam; contours) and geopotential height anomalies (m; shading), (b) 500-hPa geopotential heights (dam; contours) and geopotential height anomalies and (c) surface temperature anomalies all from 1 December 2013 through 31 March 2014. Stippling represents 90% significance based on the Student's *t*-test.

4. Discussion and Conclusion

Our case study of the winter of 2013/2014 supports that a less-discussed mode of SPV variability—SPV stretching related to wave reflection—was related to the extreme North American cold observed that winter.

The source of the wave energy that causes SPV stretching and amplification of the tropospheric standing wave over North America is the troposphere, which based on our analysis originates over Asia and then propagates eastward and upward consistent with previous studies (Kodera et al., 2008, 2013; Kretschmer, Cohen, et al., 2018; Matthias and Kretschmer, 2020). However, due to a reflective layer in the stratosphere, the upward and eastward propagating wave energy is redirected downward over the eastern North Pacific, North America and even the North Atlantic. Convergence of wave energy directed downward in the stratosphere with tropospheric wave energy over the eastern North Pacific and western North America amplifies a pre-existing tropospheric ridge in the general region of Alaska and the Gulf of Alaska (Figure S11 in Supporting Information S1). The source of the wave energy originates in the troposphere and therefore tropospheric processes are critical for reflection/SPV stretching events.

More generally, the present analysis expands our knowledge of the linkages between SPV variability and North American weather and suggests that the mechanisms highlighted in this study may improve subseasonal predictability of severe winter weather. Figure 10 summarizes the findings of our analysis. The atmospheric circulation exhibits ridging near the Scandinavia/Urals/Barents-Kara Seas and Gulf of Alaska/Alaska with troughing/low pressure in Siberia/central Asia and from central Canada into the North Atlantic region (Figure S11a–S11b in Supporting Information S1). This pattern projects strongly on a wave-2 pattern that generates wave energy that can propagate vertically from the troposphere to the stratosphere (Garfinkel et al., 2010; Martius et al., 2009; Smith et al., 2011). Amplification of the Eurasian wave consisting of Ural ridging and east Asian troughing excites anomalous wave energy that propagates both horizontally and vertically. Wave breaking in the stratosphere decelerates the zonal winds, resulting in a decrease of stratospheric zonal winds with height. This change in the vertical wind profile creates a reflective surface, and the subsequent waves are reflected back down into the troposphere. Our analysis suggests that the reflected waves converge with tropospheric wave energy in the North American sector, strengthening the Alaska ridge and resulting in overall wave amplification. Amplification of the North American standing wave subsequently increases the probability of severe winter weather across North America east of the Rockies (Figure 10). Understanding the potential tropospheric precursor of stretched SPV events remains an important research question.

This study contributes to a larger body of evidence (e.g., Cohen et al., 2021; Kretschmer, Cohen, et al., 2018; Matthias and Kretschmer, 2020) showing that SPV stretching forced by wave energy originating in the troposphere and reflecting in the stratosphere is a key driver of US cold extremes. Potential relations between severe cold air outbreaks associated with wave reflection and other known drivers, such as ENSO, the Madden Julian Oscillation and extratropical SSTs are as of yet not well understood and exhibit an important research gap related to US winter weather.

Future studies should focus on so-called nudging experiments (Hitchcock et al., 2022), whereby the troposphere and the stratosphere are individually "nudged" toward an observed state or climatology to diagnose the relative roles of variability in each of those layers to the resulting anomalous circulation pattern. Similar experiments could be run with different regions within the troposphere as well (e.g., tropics vs. mid-latitudes). Indeed, Kautz et al. (2020) and Davis et al. (2022) performed such experiments to diagnose the roles that SPV variability played (or did not play) on extreme cold air outbreaks across Eurasia (Kautz et al., 2020) and the central US (Davis et al., 2022). Such experimentation may also help us understand better why predictability of the wintertime extratropical stratospheric circulation is limited to 2 weeks or less in operational subseasonal prediction systems (e.g., Domeisen, Butler, et al., 2020).

Our analysis of the reflective events of the winter of 2013/2014 and those analyzed in Kretschmer, Cohen, et al. (2018), Matthias and Kretschmer (2020), and Cohen et al. (2021) differ from most previous reflective events analyzed (Dunn-Sigouin & Shaw, 2015, 2018; Lubis et al., 2016, 2018; Perlwitz and Harnik, 2003, 2004; Shaw and Perlwitz, 2013; Shaw et al., 2014) in several generalized aspects. First, previously studied reflective events are dominated by wave-1, while those during the winter of 2013/2014 are dominated by wave-2 (Harada & Hirooka, 2017). Moreover, the upward and downward WAF are shifted in time, in contrast to those during the winter of 2013/2014 which occurred nearly simultaneously and shifted in space. As such, the resultant SPV from

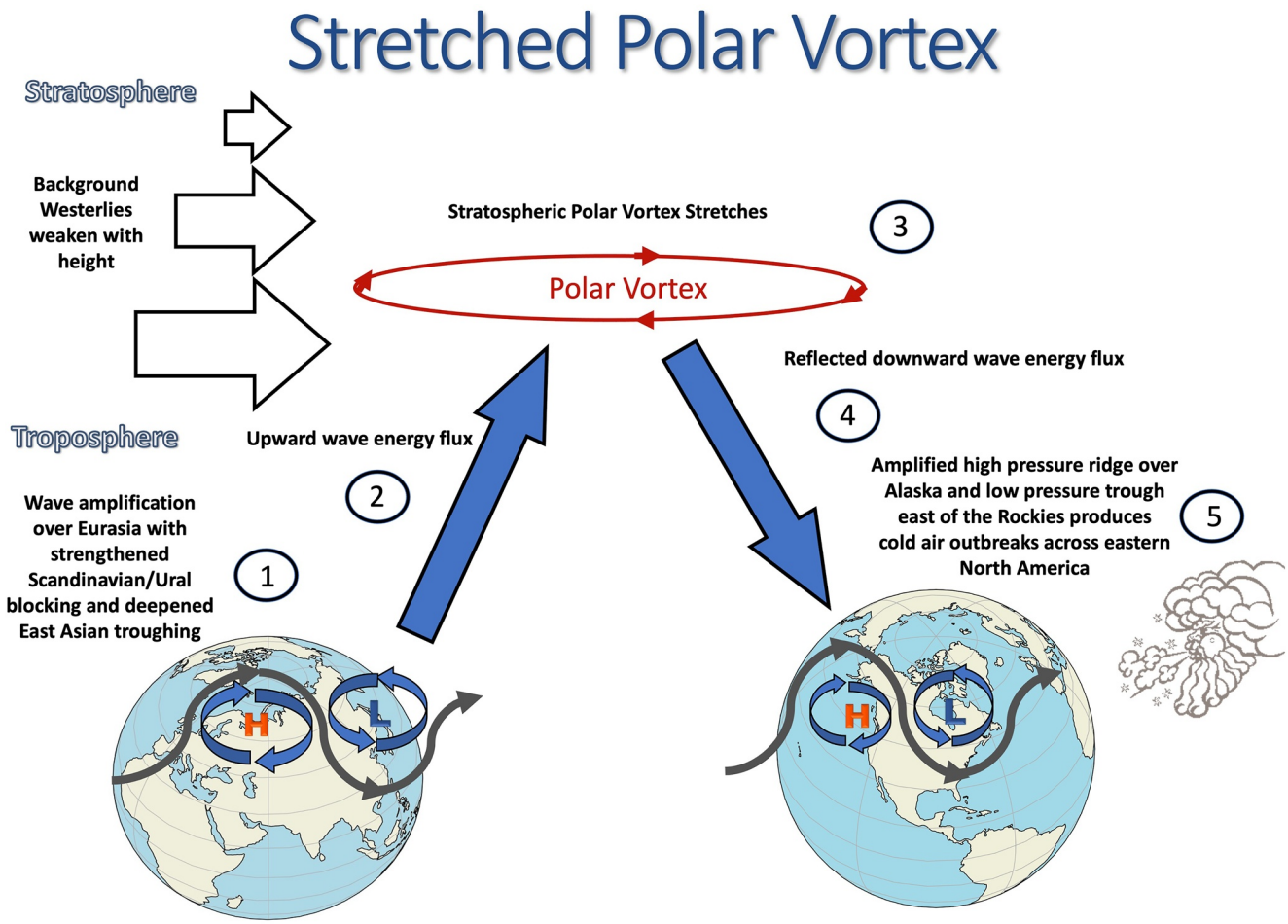

Figure 10. Idealized schematic of wave reflection mechanism based on the analysis presented. (1) Amplification of the jet stream over Eurasia with stronger Scandinavian/Ural blocking and East Asian troughing triggers, (2) increased upward atmospheric wave energy into the stratosphere. Under favorable conditions with decreasing zonal winds with height in the stratosphere, this leads to (3) a stretched stratospheric Polar Vortex (SPV) and (4) wave reflection where wave energy is directed upward over Eurasia and downward over North America. Convergence of downward wave energy in the North American sector leads to (5) wave amplification over North America with a northward shifted jet stream over the Gulf of Alaska and Alaska, a southward shifted jet stream over North America and an increase in extreme winter weather (cold and snow) across eastern North America.

the reflected wave-1 events is more circular in shape, while the SPV is stretched or elongated due to reflected wave-2. Finally, the wave-1 reflective events are associated with widespread relatively mild temperatures especially across Eurasia, in sharp contrast to the widespread cold in eastern North America and parts of Asia during the winter of 2013/2014.

Taken together, the tropospheric circulation pattern associated with stretched SPV events (i.e., anomalous ridging in the Pacific and a deep trough in central North America) have larger immediate surface impacts in terms of extreme cold temperatures across North America than major SSW events. Thus, despite their short duration relative to the more persistent influence of SSWs on the tropospheric circulation, the large magnitude of the surface impacts and the higher likelihood of repeatability, the surface influence of SPV stretching events can impact seasonal mean temperatures (Kretschmer, Cohen, et al., 2018). The unique nature of the winter of 2013/2014 led to an unusually severe winter across eastern North America not only in amplitude (Harada & Hirooka, 2017) but also duration (https://psl.noaa.gov/news/2015/110515.html).

Attribution of the occurrence of cold surface temperatures to the "polar vortex" in the winter 2013/2014 introduced confusion and even debate among scientists on the appropriateness of its colloquial usage (Waugh et al., 2017). The introduction by the media of the term "polar vortex" to a lay audience to attribute cold air outbreaks during the winter of 2013/2014 was misleading. However, our analysis illustrates a strong relationship between various

modes of SPV variability and severe winter weather during the winter of 2013/2014. The adoption by the media of the term "polar vortex" during that winter, in retrospect, has unintentionally highlighted related SPV variability to severe winter weather heretofore not widely appreciated even among scientists.

Data Availability Statement

No new data sets were created in the drafting of the manuscript. ERA5 data is available for download from: https://www.ecmwf.int/en/forecasts/datasets/reanalysis-datasets/era5.

Acknowledgments
J. Cohen is supported by the US National Science Foundation grants AGS-1657748, PLR-1901352, and AGS-2140909. J. C. Furtado is supported by the US National Science Foundation grant AGS-1657905. M. K. has received funding from the European Union's Horizon 2020 research and innovation programme under the Marie Skłodowska-Curie grant agreement [No 841902].

References

ABC News. (2014). Retrieved from https://abcnews.go.com/US/polar-vortex-misused-weather-term-2014/story?id=26793261
AIR. (2014). Retrieved from https://www.air-worldwide.com/blog/posts/2014/4/the-winter-of-20132014-dont-blame-the-polar-vortex/
Baldwin, M. P. (2001). Annular modes in global daily surface pressure. *Geophysical Research Letters*, *28*(21), 4115–4118. https://doi.org/10.1029/2001gl013564
Baldwin, M. P., & Dunkerton, T. J. (1999). Propagation of the Arctic Oscillation from the stratosphere to the troposphere. *Journal of Geophysical Research*, *104*(D24), 30937–30946. https://doi.org/10.1029/1999JD900445
Baldwin, M. P., & Dunkerton, T. J. (2001). Stratospheric harbingers of anomalous weather regimes. *Science*, *294*(5542), 581–584. https://doi.org/10.1126/science.1063315
Baxter, S., & Nigam, S. (2015). Key role of the North Pacific Oscillation–West Pacific pattern in generating the extreme 2013/14 North American winter. *Journal of Climate*, *28*(20), 8109–8117. https://doi.org/10.1175/JCLI-D-14-00726.1
Butler, A. H., Seidel, D. J., Hardiman, S. C., Butchart, N., Birner, T., & Match, A. (2015). Defining sudden stratospheric warmings. *Bulletin of the American Meteorological Society*, *96*(11), 1913–1928. https://doi.org/10.1175/bams-d-13-00173.1
Butler, A. H., Sjoberg, J. P., Seidel, D. J., & Rosenlof, K. H. (2017). A sudden stratospheric warming compendium. *Earth System Science Data*, *9*(1), 63–76. https://doi.org/10.5194/essd-9-63-2017
CBS News. (2014). Retrieved from https://www.cbsnews.com/pictures/the-polar-vortex-of-2014
Charlton, A. J., & Polvani, L. M. (2007). A new look at stratospheric sudden warmings. Part I: Climatology and modeling benchmarks. *Journal of Climate*, *20*(3), 449–469. https://doi.org/10.1175/JCLI3996.1
Charney, J. G., & Drazin, P. G. (1961). Propagation of planetary-scale disturbances from the lower into the upper atmosphere. *Journal of Geophysical Research*, *66*(1), 83–109. https://doi.org/10.1029/JZ066i001p00083
Cohen, J., Agel, L., Barlow, M., Garfinkel, C. I., & White, I. (2021). Linking Arctic variability and change with extreme winter weather in the US. *Science*, *373*(6559), 1116–1121. https://doi.org/10.1126/science.abi9167
Cohen, J., Ye, H., & Jones, J. (2015). Trends and variability in rain-on-snow events. *Geophysical Research Letters*, *42*(17), 7115–7122. https://doi.org/10.1002/2015GL065320
Cohen, J., Zhang, X., Francis, J., Jung, T., Kwok, R., Overland, J., et al. (2020). Divergent consensuses on Arctic amplification influence on mid-latitude severe winter weather. *Nature Climate Change*, *10*(1), 20–29. https://doi.org/10.1038/s41558-019-0662-y
Davis, N. A., Richter, J. H., Glanville, A. A., Edwards, J., & LaJoie, E. (2022). Limited surface impacts of the January 2021 sudden stratospheric warming. *Nature Communications*, *13*(1), 1136. https://doi.org/10.1038/s41467-022-28836-1
Dole, R., & Gordon, N. (1983). Persistent anomalies of the extratropical Northern Hemisphere wintertime circulation: Geographical distribution and regional persistence characteristics. *Monthly Weather Review*, *111*(8), 1567–1586. https://doi.org/10.1175/1520-0493(1983)111<1567:paoten>2.0.co;2
Domeisen, D. I. V., Butler, A. H., Charlton-Perez, A. J., Ayarzagüena, B., Baldwin, M. P., Dunn-Sigouin, E., et al. (2020). The role of the stratosphere in subseasonal to seasonal prediction: 1. Predictability of the stratosphere. *Journal of Geophysical Research: Atmospheres*, *125*, e2019JD030920. https://doi.org/10.1029/2019JD030920
Domeisen, D. I. V., Grams, C. M., & Papritz, L. (2020). The role of North Atlantic–European weather regimes in the surface impact of sudden stratospheric warming events. *Weather and Climate Dynamics*, *1*(2), 373–388. https://doi.org/10.5194/wcd-1-373-2020
Dunn-Sigouin, E., & Shaw, T. (2018). Dynamics of extreme stratospheric negative heat flux events in an idealized model. *Journal of the Atmospheric Sciences*, *75*(10), 3521–3540. https://doi.org/10.1175/jas-d-17-0263.1
Dunn-Sigouin, E., & Shaw, T. A. (2015). Comparing and contrasting extreme stratospheric events, including their coupling to the tropospheric circulation. *Journal of Geophysical Research: Atmospheres*, *120*, 1374–1390. https://doi.org/10.1002/2014jd022116
ESRL. (2020). Retrieved from https://www.esrl.noaa.gov/csl/groups/csl8/sswcompendium/majorevents.html
Garfinkel, C. I., Hartmann, D. L., & Sassi, F. (2010). Tropospheric precursors of anomalous Northern Hemisphere stratospheric polar vortices. *Journal of Climate*, *23*(12), 3282–3299. https://doi.org/10.1175/2010jcli3010.1
Gelaro, R., McCarty, W., Suarez, M. J., Todling, R., Molod, A., Takacs, L., et al. (2017). The modern-era retrospective analysis for research and applications, version 2 (MERRA-2). *Journal of Climate*, *30*(14), 5419–5454. https://doi.org/10.1175/jcli-d-16-0758.1
Gong, D., & Wang, S. (1999). Definition of the Antarctic Oscillation index. *Geophysical Research Letters*, *26*(4), 459–462. https://doi.org/10.1029/1999gl900003
Harada, Y., & Hirooka, T. (2017). Extraordinary features of the planetary wave propagation during the boreal winter 2013/2014 and the zonal wavenumber two predominance. *Journal of Geophysical Research: Atmospheres*, *122*, 11374–11387. https://doi.org/10.1002/2017JD027053
Harnik, N. (2009). Observed stratospheric downward reflection and its relation to upward pulses of wave activity. *Journal of Geophysical Research*, *114*, D08120. https://doi.org/10.1029/2008jd010493
Harnik, N., & Lindzen, R. S. (2001). The effect of reflecting surfaces on the vertical structure and variability of stratospheric planetary waves. *Journal of the Atmospheric Sciences*, *58*(19), 2872–2894. https://doi.org/10.1175/1520-0469(2001)058<2872:teorso>2.0.co;2
Hartmann, D. L. (2015). Pacific sea surface temperature and the winter of 2014. *Geophysical Research Letters*, *42*(6), 1894–1902. https://doi.org/10.1002/2015gl063083
Hersbach, H., Bell, B., Berrisford, P., Hirahara, S., Horanyi, A., Munoz-Sabater, J., et al. (2020). The ERA5 global reanalysis. *Quarterly Journal of the Royal Meteorological Society*, *146*(730), 1999–2049. https://doi.org/10.1002/qj.3803

Hitchcock, P., Butler, A., Charlton-Perez, A., Garfinkel, C., Stockdale, T., Anstey, J., et al. (2022). Stratospheric nudging and predictable surface impacts (SNAPSI): A protocol for investigating the role of the stratospheric polar vortex in subseasonal to seasonal forecasts. *Geoscientific Model Development*. in press. https://doi.org/10.5194/gmd-2021-394

Horel, J. D., & Wallace, J. M. (1981). Planetary-scale atmospheric phenomena associated with the Southern Oscillation. *Monthly Weather Review*, *109*(4), 813–829. https://doi.org/10.1175/1520-0493(1981)109<0813:psapaw>2.0.co;2

Kautz, L., Polichtchouk, I., Birner, T., Garny, H., & Pinto, J. (2020). Enhanced extended-range predictability of the 2018 late-winter Eurasian cold spell due to the stratosphere. *Quarterly Journal of the Royal Meteorological Society*, *146*(727), 1040–1055. https://doi.org/10.1002/qj.3724

Kodera, K., Mukougawa, H., & Fujii, A. (2013). Influence of the vertical and zonal propagation of stratospheric planetary waves on tropospheric blockings. *Journal of Geophysical Research: Atmospheres*, *118*, 8333–8345. https://doi.org/10.1002/jgrd.50650

Kodera, K., Mukougawa, H., & Itoh, S. (2008). Tropospheric impact of reflected planetary waves from the stratosphere. *Geophysical Research Letters*, *35*(16), L16806. https://doi.org/10.1029/2008gl034575

Kodera, K., Mukougawa, H., Maury, P., Ueda, M., & Claud, C. (2016). Absorbing and reflecting sudden stratospheric warming events and their relationship with tropospheric circulation. *Journal of Geophysical Research: Atmospheres*, *121*, 80–94. https://doi.org/10.1002/2015jd023359

Kretschmer, M., Cohen, J., Matthias, V., Runge, J., & Coumou, D. (2018). The different stratospheric influences on cold extremes in Eurasia and North America. *npj Climate and Atmospheric Science*, *1*, 44. https://doi.org/10.1038/s41612-018-0054-4

Kretschmer, M., Coumou, D., Angel, L., Barlow, M., Tziperman, E., & Cohen, J. (2018). More-persistent weak stratospheric polar vortex states linked to cold extremes. *Bulletin of the American Meteorological Society*, *99*(1), 46–60. https://doi.org/10.1175/BAMS-D-16-0259.1

Lee, S. H., Furtado, J. C., & Charlton-Perez, A. J. (2019). Wintertime North American weather regimes and the Arctic stratospheric polar vortex. *Geophysical Research Letters*, *46*(24), 14892–14900. https://doi.org/10.1029/2019GL085592

Linkin, M. E., & Nigam, S. (2008). The North Pacific Oscillation-West Pacific teleconnection pattern: Mature-phase structure and winter impacts. *Journal of Climate*, *21*(9), 1979–1997. https://doi.org/10.1175/2007jcli2048.1

Lubis, S. W., Matthes, K., Harnik, N., Omrani, N., & Wahl, S. (2018). Downward wave coupling between the stratosphere and troposphere under future anthropogenic climate change. *Journal of Climate*, *31*(10), 4135–4155. https://doi.org/10.1175/jcli-d-17-0382.1

Lubis, S. W., Matthes, K., Omrani, N., Harnik, N., & Wahl, S. (2016). Influence of the quasi-biennial oscillation and sea surface temperature variability on downward wave coupling in the Northern Hemisphere. *Journal of the Atmospheric Sciences*, *73*(5), 1943–1965. https://doi.org/10.1175/jas-d-15-0072.1

Manney, G. L., Butler, A. H., Lawrence, Z. D., Wargan, K., & Santee, M. L. (2022). What's in a name? On the use and significance of the term "polar vortex". *Geophysical Research Letters*, *49*(10), e2021GL097617. https://doi.org/10.1029/2021GL097617

Martius, O., Polvani, L. M., & Davies, H. C. (2009). Blocking pre-cursors to stratospheric sudden warming events. *Geophysical Research Letters*, *36*(14), L14806. https://doi.org/10.1029/2009GL038776

Matsuno, T. (1970). Vertical propagation of stationary planetary waves in the winter Northern Hemisphere. *Journal of the Atmospheric Sciences*, *27*(6), 871–883. https://doi.org/10.1175/1520-0469(1970)027<0871:VPOSPW>2.0.CO;2

Matthias, V., & Kretschmer, M. (2020). The influence of stratospheric wave reflection on North American cold spells. *Monthly Weather Review*, *148*(4), 1675–1690. https://doi.org/10.1175/MWR-D-19-0339.1

Namias, J. (1950). The index cycle and its role in the general circulation. *Journal of the Atmospheric Sciences*, *7*(2), 130–139. https://doi.org/10.1175/1520-0469(1950)007<0130:ticair>2.0.co;2

Nath, D., Chen, W., Wang, L., & Ma, Y. (2014). Planetary wave reflection and its impact on tropospheric cold weather over Asia during January 2008. *Advances in Atmospheric Sciences*, *31*(4), 851–862. https://doi.org/10.1007/s00376-013-3195-8

NOAA. (2014). Retrieved from https://www.weather.gov/safety/cold-polar-vortex

NWS. (2014). Retrieved from https://www.weather.gov/lot/coldest_dec_to_march

NY Times. (2019). Retrieved from https://www.nytimes.com/2019/01/18/climate/polar-vortex-2019.html

Perlwitz, J., & Harnik, N. (2003). Observational evidence of a stratospheric influence on the troposphere by planetary wave reflection. *Journal of Climate*, *16*(18), 3011–3026. https://doi.org/10.1175/1520-0442(2003)016<3011:oeoasi>2.0.co;2

Perlwitz, J., & Harnik, N. (2004). Downward coupling between the stratosphere and troposphere: The relative roles of wave and zonal mean processes. *Journal of Climate*, *17*(24), 4902–4909. https://doi.org/10.1175/JCLI-3247.1

Plumb, R. (1985). On the three-dimensional propagation of stationary waves. *Journal of the Atmospheric Sciences*, *42*(3), 217–229. https://doi.org/10.1175/1520-0469(1985)042<0217:OTTDPO.2.0.CO;2

Plumb, R. A. (1986). Three-dimensional propagation of transient quasi-geostrophic eddies and its relationship with the eddy forcing of the time-mean flow. *Journal of the Atmospheric Sciences*, *43*(16), 1657–1678. https://doi.org/10.1175/1520-0469(1986)043<1657:TDPOTQ>2.0.CO;2

Polvani, L. M., & Kushner, P. J. (2002). Tropospheric response to stratospheric perturbations in a relatively simple general circulation model. *Geophysical Research Letters*, *29*(7), 1114. https://doi.org/10.1029/2001GL014284

Rogers, J. C. (1981). The North Pacific oscillation. *Journal of Climatology*, *1*, 39–57. https://doi.org/10.1002/joc.3370010106

Shapiro, M. A., Hampel, T., & Krueger, A. J. (1987). The Arctic tropopause fold. *Monthly Weather Review*, *115*(2), 444–454. https://doi.org/10.1175/1520-0493(1987)115<0444:TAFF>2.0.CO;2

Shaw, T. A., & Perlwitz, J. (2013). The life cycle of Northern Hemisphere downward wave coupling between the stratosphere and troposphere. *Journal of Climate*, *26*(5), 1745–1763. https://doi.org/10.1175/jcli-d-12-00251.1

Shaw, T. A., Perlwitz, J., & Harnik, N. (2010). Downward wave coupling between the stratosphere and troposphere: The importance of meridional wave guiding and comparison with zonal-mean coupling. *Journal of Climate*, *23*, 6365–6381. https://doi.org/10.1175/2010JCLI3804.1

Shaw, T. A., Perlwitz, J., & Weiner, O. (2014). Troposphere-stratosphere coupling: Links to North Atlantic weather and climate, including their representation in CMIP5 models. *Journal of Geophysical Research: Atmospheres*, *119*, 5864–5880. https://doi.org/10.1002/2013jd021191

Sigmond, M., & Fyfe, J. (2016). Tropical Pacific impacts on cooling North American winters. *Nature Climate Change*, *6*(10), 970–974. https://doi.org/10.1038/nclimate3069

Singh, D., Swain, D. L., Mankin, J. S., Horton, D. E., Thomas, L. N., Rajaratnam, B., & Diffenbaugh, N. S. (2016). Recent amplification of the North American winter temperature dipole. *Journal of Geophysical Research: Atmospheres*, *121*, 9911–9928. https://doi.org/10.1002/2016JD025116

Sjoberg, J. P., & Birner, T. (2012). Transient tropospheric forcing of sudden stratospheric warmings. *Journal of the Atmospheric Sciences*, *69*(11), 3420–3432. https://doi.org/10.1175/JAS-D-11-0195.1

Smith, K., Kushner, P. J., & Cohen, J. (2011). The role of linear interference in Northern Annular Mode variability associated with Eurasian snow cover extent. *Journal of Climate*, *24*(23), 6185–6202. https://doi.org/10.1175/jcli-d-11-00055.1

Thompson, D. W. J., Baldwin, M. P., & Wallace, J. M. (2002). Stratospheric connection to Northern Hemisphere wintertime weather: Implications for prediction. *Journal of Climate*, *15*(12), 1421–1428. https://doi.org/10.1175/1520-0442(2002)015<1421:sctnhw>2.0.co;2

Thompson, D. W. J., & Wallace, J. M. (1998). The Arctic oscillation signature in the wintertime geopotential height and temperature fields. *Geophysical Research Letters*, *25*(9), 1297–1300. https://doi.org/10.1029/98gl00950

Thompson, D. W. J., & Wallace, J. M. (2000). Annular modes in the extratropical circulation. Part I: Month-to-month variability. *Journal of Climate*, *13*(5), 1000–1016. https://doi.org/10.1175/1520-0442(2000)013<1000:amitec>2.0.co;2

Thompson, D. W. J., & Wallace, J. M. (2001). Regional climate impacts of the Northern Hemisphere annular mode. *Science*, *293*(5527), 85–89. https://doi.org/10.1126/science.1058958

Tibaldi, S., & Molteni, F. (1990). On the operational predictability of blocking. *Tellus*, *42A*(3), 343–365. https://doi.org/10.3402/tellusa.v42i3.11882

Waugh, D., Sobel, A., & Polvani, L. (2017). What is the polar vortex and how does it influence weather? *Bulletin of the American Meteorological Society*, *98*(1), 37–44. https://doi.org/10.1175/BAMS-D-15-00212.1